

Measurements and simulations of diamond detector response to radiation.

E. Alemanno^{1, 2}, A. Caricato^{1, 2}, G. Chiodini¹, M. Corrado^{1, 2}, G. Fiore¹, M. Martino^{1, 2}, R. Perrino¹, C. Pinto^{1, 2} and S. Spagnolo^{1, 2}, for the DIAPIX collaboration.

¹Istituto Nazionale di Fisica Nucleare, Sezione di Lecce, Italy.

²Dipartimento di Fisica, Università del Salento, Italy.

We acquired from Diamond Detectors Ltd several detector-grade diamond sensors in order to understand and simulate in great details the response to radioactive sources with and without an external magnetic field. In fact, we realized several detector configuration:

Detector-I : One 5x5 mm², 0.3 mm thick, poly-crystal sensor metallized on both sides with a large pad.

Detector-II : One 5x5 mm², 0.3 mm thick, poly-crystal sensor laser graphitized on both sides with a large pad.

Detector-III : Two 10x10 mm², 0.5 mm thick, poly-crystal sensor metallized on the front-side with four 1.5 mm pitch strips and on the back-side with a large pad.

Detector-IV : One 4.7x4.7 mm², 0.5 mm thick, mono-crystal sensor metallized on the front-side with two 1.5 mm pitch strips and on the back-side with a large pad.

Detector-V : Three 8x8 mm², 0.5 mm thick, poly-crystal sensor metallized on the front-side with 32 by 128 pixel cells and on the back-side with a large pad.

The three pixel detector IV were sent to IZM Berlin for the pixel matrix and back-plane metallization and for the bump-bonding to superPIX0 readout chip. In order to employ the superPIX0 chip we signed an agreement with the superB collaboration which is extremely interested to evaluate the pixel diamond detector with such a small readout pitch. These detectors are under test in Lecce with pattern generator and logic analyzer setup on a bench test.

Detectors I,II, and III were readout by a traditional Ortec 142 A charge sensitive preamplifier and the signal output passed to an Ortec 570 shaping amplifier followed by a multichannel analyzer for the pulse height spectra acquisition. We used detector I to measure the response

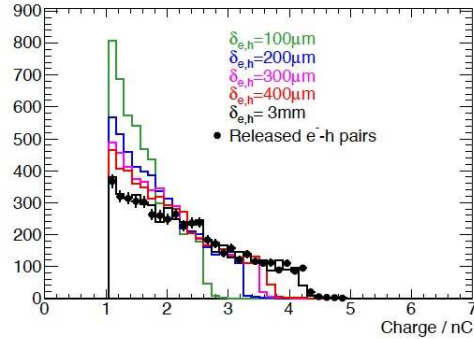


Figure 1. Simulations with GEANT4 of the response of a detector-grade poly-crystal diamond to a ²²Na γ -source.

of poly-crystal diamond to α , β , and γ radiation. We used all three type of radiation because they gives complementary informations. The α radiation stops 12 μm after crossing the diamond surface. The β radiation crosses all diamond bulk and can mimic the energy release of a minimum ionizing particle. Finally, the γ radiation creates mostly short-path low-energy Compton electrons uniformly along the diamond bulk depth.

We simulated the charge distribution released in diamond by the above mentioned radioactive sources using the simulation software Geant4. In order to compare with the measured spectra we evaluate the elementary induced charge q_{ind} by the elementary released charge q_{rel} using the Hecht's equation:

$$q_{ind} = Q_{rel} \frac{l_i}{d} (1 - e^{-\frac{d}{l_i}}), \quad (1)$$

where d is the detector thickness, l_i is the mean free path of the free carrier of type i due to trapping or recombination phenomena. The mean free path is related to the free carrier lifetime $\tau_{e,h}$ by the formula $l_{e,h} = v_{e,h} \tau_{e,h}$, where $v_{e,h}$ is the drift velocity.

We are comparing the measured β , α e γ spectra of a detector-grade poly-crystal diamond and we are not yet able to reproduce all the results with the simulations assuming an unique average

collected charge given by $Q_{ind} = Q_{rel} \frac{CCD}{d} [1 - \frac{CCD}{d} (1 - e^{-\frac{d}{\tau_{col}}})]$ from the β spectra, where CCD is called Charge Collection Distance and is about $350 \mu\text{m}$ for the best poly-crystal diamond. In fact, trapping and recombination centers, due to impurity and lattice imperfection, reduce the free carriers lifetime.

The most difficult data to reproduce by simulation are the γ spectra. Figure 1 shows the expected collected charge by a poly-crystal diamond sensor $300 \mu\text{m}$ thick for different values of CCD irradiated by a ^{22}Na γ -source. It is possible to notice that the Compton shoulder in the spectra is clearly visible also for CCD much shorter the sensor thickness contrary to the observation. Instead, irradiating mono-crystal diamond detector with γ -sources the Compton shoulder is clearly visible and a monochromatic α spectra is evident, showing that for mono-crystal diamond sensor the CCD is much larger than sensor thickness and the charge collection is 100% efficient.

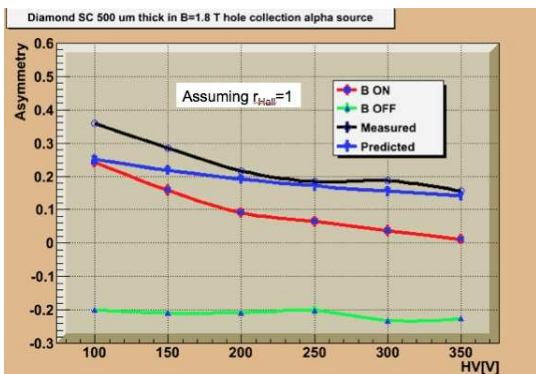


Figure 2. Measured and simulated charge-sharing asymmetry of 0.5 mm collimated ^{241}Am α -source for mono-crystal strip diamond detector with and without 1.8 T magnetic field as a function of the electric field.

We used detector III and IV to studies charge-sharing phenomena between adjacent strip with and without magnetic field. We performed these measurements at CERN in Ginevra where we have available a room temperature dipole magnet with big aperture assigned to us by the Normal Conducting Magnet division. The magnet can generate a magnetic field up to about 1.8 Tesla in a relative large aperture. We placed our detector, the first stage of the electronics, and the α source inside the magnet. The α particle bending in magnetic field between the collimator aperture end and the detector is simulated by Geant4.

In order to simulate the charge-sharing is necessary to evaluate in details the carriers movements,

the induced signal in complex electrodes configuration, trapping-recombination, and diffusion phenomena. We implemented several MATHLAB scripts to solve each problem in a modular way. In particular, we solved the Poisson equation to evaluated the drift field and the weighting field using the Partial Differential Equation solver.

To measure charge-sharing we placed the collimated source on the detector back-side below two adjacent strips (named 2 and 3) and measured the pair of induced pulse heights (Q_2 and Q_3). Charge-sharing is defined by events with both collected charges above a threshold of about 10,000 electrons. The relation between the beam spot position and the charge-sharing asymmetry, defined by $A = \frac{Q_2 - Q_3}{Q_2 + Q_3}$, is expect highly nonlinear. The extraction of the Lorentz angle in magnetic field is possible only if the simulations are very reliable.

To verify the correctness of the methodology and of the simulations we repeated the same measurements with mono-crystal detector with two readout strip with spatial separation similar to poly-crystal detector. A detector-grade mono-crystal diamond can collect all generated charge and the charge-sharing measurements should be easier to interpret making sure that the systematic errors are under control.

In Figure 3 the charge-sharing asymmetry is plotted for the case of mono-crystal diamond strip detector as a function of the electric field and with or without magnetic field. Measurements deviate from simulations for low electric field where polarization phenomena can alter significantly the internal field with respect to the applied one.

In the literature irradiation test of diamond detector with a non relativistic 25 MeV proton beam is also reported [3], showing a quite controversial performance degradation with respect to ultra-relativistic proton beam. The energy spectra of the radiation field expected near the interaction region and near the beam in the forward region at collider experiment extend up to very low energy. For this reason, diamond radiation damage data with non relativistic proton of different anergy and from different groups are very useful.

We irradiated two diamond detectors with 62 MeV energy proton beam up to an integrated fluence of about 2×10^{15} protons/cm² at INFN-LNS in Catania (Italy). The detectors were made by two high purity poly-crystal diamond sensors. The electric contacts of the two diamond sensors were from different sources and made with different techniques: a proprietary DLC/Pt/Au electric contact and our own novel UV Laser technique. We measured the detector pulse height before and after irradiation using proton beams and a fast charge sensitive amplifier. The fast charge

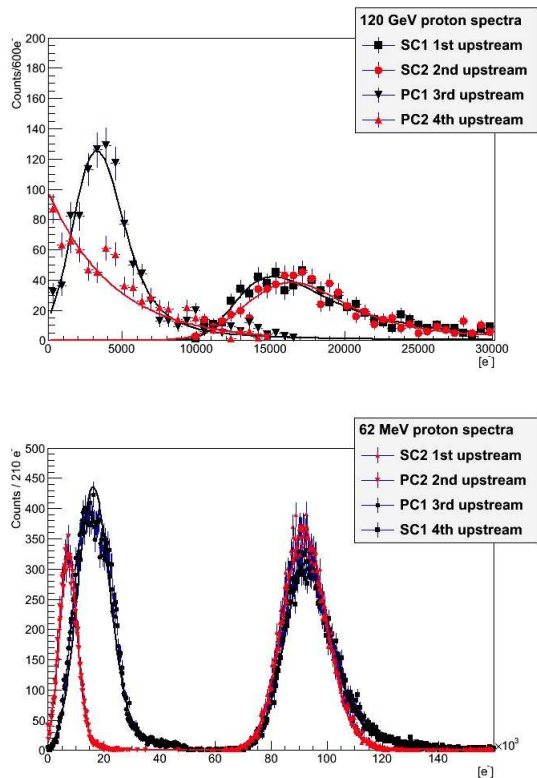


Figure 3. Charge distribution collected by diamond detectors due to the crossing of 120 GeV protons (upper plots) and 62 MeV protons (lower plots) after irradiation of PC detectors. The data correspond to an applied voltage of +300V. The fit correspond to a Landau distribution convoluted with a Gaussian function.

sensitive amplifier gains were equalized by measuring the response to the same electrical pulse. The radiation damage was quantified in terms of the relative charge collection efficiency drop.

The beam relative fluence was continuously measured during the irradiation by the current drawn by a Secondary Electron Emission (SEE) device. The SEE device was made by a Tantalum foil and intercepted the beam in vacuum 5 cm before the transition in air made by a kapton foil to irradiate the diamond samples. The diamond samples were placed in line around the beam line with the pc-board with the photodiode device, 2 cm downstream the irradiation beam. The diamond sensors were irradiated with zero bias polarization, while the photodiodes were left floating.

The relative fluence values were converted in absolute fluence values by calibrating the SEE current by a beam current scan before starting the irradiation. Finally, the beam profile was measured along X and Y by a high dose Gafchromic

film exposed for few seconds to the beam and carefully aligned with the samples to irradiated. The analysis was made off-line by a photographic scanner. With this method we found a transversal beam radius of about 25 mm at 10% and 15 mm at 90% from the maximum intensity which was centered in front of our targets.

The detector response is measured with proton beams and using a fast charge amplifier. Landau peak separation from noise is possible for relativistic protons only before irradiation for this reason after irradiation we used the 62 MeV protons, the same used for the irradiation test, which release in diamond a charge 5.5 times bigger than minimum ionizing particles. The rise-time is dominated by Front-End electronics. No change in pulse shape observed before and after irradiation.

In Figure 3 the Charge distribution collected by diamond detectors due to the crossing of 120 GeV protons (upper plots) and 62 MeV protons (lower plots) after irradiation of PC detectors. The CCD of the poly-crystal diamond detectors can be evaluated from the ratio between the poly-crystal and the mono-crystal average pulse height after calibration and assuming a full charge collection for the 500 μm thick mono-crystal sensor. From the upper plots a 113 μm CCD for the PC1 detector can be extracted and a 10% drop after irradiation can be estimated from the lower plot. For the PC2 detector the quite small CCD before irradiation couldn't be evaluated and only the CCD after the irradiation can be estimated to be about . This is possible because after irradiation we used the 62 MeV proton generated charge which is 5.26 times larger than a MIP and a value 41 μm .

REFERENCES

1. "Radiation detectors based on synthetic diamond", Alemanno E, Caricato A, Chiodini G, Martino M, Perrino R, Spagnolo S. IL NUOVO CIMENTO C, vol. 36, p. 61-65, ISSN: 2037-4909, doi: 10.1393/ncc/i2013-11408-7 (2012).
2. "Radiation damage of polycrystalline diamond exposed to 62 MeV proton beam", G. Chiodini et al. 9th International Conference on Radiation Effects on Semiconductor Materials Detectors and Devices. October 9-12, Florence Italy
3. "Radiation hardness of diamond and silicon sensors compared" Win de Boer et al., Phys. Status Solidi 204:3009 (2007).